JNeurosci
THE JOURNAL OF NEUROSCIENCE

Research Articles | Systems/Circuits

State-Dependent Modulation of Corticospinal and Cortical Responses by Closed-Loop Paired-pulse TMS

https://doi.org/10.1523/JNEUROSCI.0762-26.2026

Received: 5 May 2026
Revised: 5 October 2026
Accepted: 8 October 2026

Copyright © 2026 the authors

This Early Release article has been peer reviewed and accepted, but has not been through the composition and copyediting processes.The final version may differ slightly in style or formatting and will contain links to any extended data.

Alerts: Sign up at www.jneurosci.org/alerts to receive customized email alerts when the fully formatted version of this article is published.

State-Dependent Modulation of Corticospinal and Cortical Responses by Closed-Loop Paired-pulse TMS

Abbreviated title: Phase-Dependent Paired-pulse TMS Responses

Da Som Choi[1], Malte R. Güth[1], Michelle Ma[1], Makaha Harmon[1], Miles Wischnewski[2], Jimin Park[1], Aneka Blenker[1], Sangjun Lee[1], Alexander Opitz[1*]

[1] Department of Biomedical Engineering, University of Minnesota, Minneapolis, MN 55455, USA

[2] Department of Experimental Psychology, University of Groningen, Groningen 9712TS, Netherlands

* Corresponding author, aopitz@umn.edu

Author Contributions: D.C., M.R.G., M.W., and A.O. designed research; D.C., M.R.G., M.M., M.H., J.P., and A.B. performed research; D.C., M.R.G., and S.L. contributed unpublished reagents/analytic tools; D.C. and S.L. analyzed data; D.C. wrote the first draft of the paper; D.C., M.R.G., S.L., and A.O. edited the paper; D.C. wrote the paper.

Number of pages: 23

Number of figures: 4

Number of tables: 4

Number of words for abstract: 250

Number of words for introduction: 597

Number of words for discussion: 1500

JNeurosci Accepted Manuscript

Conflict of interest: The authors declare no competing financial interests.

Acknowledgments: This research was supported by the University of Minnesota's MnDRIVE (Minnesota's Discovery, Research and Innovation Economy) initiative and National Science Foundation (NSF) Career Grant (2143852).

JNeurosci Accepted Manuscript

Abstract

Brain oscillations shape cortical excitability in a phase-dependent manner. Cortical excitability reflects the net output of intracortical circuits, including inhibitory and facilitatory pathways. However, whether the phase of ongoing brain rhythms differentially modulates inhibitory and facilitatory responses remains unknown. Paired-pulse transcranial magnetic stimulation (ppTMS) can selectively engage these circuits, providing a unique tool to dissociate their contributions. We combined real-time EEG-guided closed-loop TMS with single- and paired-pulse TMS in 24 healthy adults (13 female) to probe how sensorimotor mu (8–13 Hz) and beta (14–30 Hz) oscillatory phase shapes responses associated with intracortical inhibitory and facilitatory processes. Single-pulse TMS (spTMS), short-interval intracortical inhibition (SICI), and intracortical facilitation (ICF) were delivered at four phases (peak, falling, trough, rising). Motor evoked potentials (MEPs) and TMS-evoked potentials (TEPs) were recorded to assess corticospinal and cortical responses, respectively. We found that MEP amplitude was phase-dependent across all three stimulation types, with spTMS-evoked and ICF-conditioned MEPs showing the largest amplitudes at the rising phase, whereas SICI-conditioned MEPs were largest at the peak phase of the mu oscillation. TEP P60-N100 amplitude was modulated by oscillatory phase across all stimulation types, with maximal responses at the trough phase. SICI showed opposing phase patterns between the two measures, revealing a dissociation between cortical and corticospinal responses. MEP and TEP preferred phases were correlated across participants only in the ICF condition. These findings extend phase-dependent spTMS effects to paired-pulse stimulation and show that ongoing mu phase differentially shapes responses to SICI and ICF across cortical and corticospinal levels.

Significance Statement

Ongoing brain oscillations are known to shape cortical excitability across their phase cycle. However, whether this effect differentially influences inhibitory and facilitatory responses has remained unresolved. Here, using closed-loop EEG-guided transcranial magnetic stimulation in healthy adults, we probed how SICI- and ICF-conditioned responses vary across different phases of the sensorimotor mu and beta rhythms. We show that corticospinal and cortical responses to inhibitory and facilitatory paired-pulse protocols exhibit distinct phase-dependent patterns in the sensorimotor mu rhythm. These

JNeurosci Accepted Manuscript

findings extend phase-dependent stimulation effects beyond single-pulse TMS and reveal that the relationship between cortical state and stimulation response differs across paired-pulse protocols.

JNeurosci Accepted Manuscript

Introduction

Transcranial magnetic stimulation (TMS) is a noninvasive brain stimulation technique that modulates neuronal activity by inducing electric fields in targeted brain regions (Siebner et al., 2022). TMS can thereby probe cortical excitability in a causal and spatially precise manner. Cortical activity is characterized by ongoing neural oscillations across multiple frequency bands (Buzsáki & Draguhn, 2004). The phase of these oscillations reflects cyclical fluctuations in neuronal excitability, such that different phases correspond to distinct excitability states. Consequently, TMS responses are systematically shaped by the oscillatory phase at the moment of stimulation, referred to as phase-dependent modulation (Dugué et al., 2011; Wischnewski et al., 2024).

Recent advances have enabled the use of electroencephalography (EEG) to estimate the phase of ongoing oscillations and deliver TMS accordingly (Chen et al., 2013; Shirinpour et al., 2020, 2025; Zrenner et al., 2018). Such closed-loop technology enables precise investigation of phase-dependent cortical excitability in humans. Closed-loop EEG-TMS has been used to deliver stimulation at specific phases of sensorimotor mu (8-13 Hz) (Bergmann et al., 2019; Schaworonkow et al., 2019; Wischnewski et al., 2022; Zrenner et al., 2018) or beta (14-30 Hz) rhythms (Haigh et al., 2025; Wischnewski et al., 2022) with motor evoked potentials (MEPs) revealing phase-dependent modulation of corticospinal excitability. In addition, TMS-evoked potentials (TEPs), reflecting cortical excitability and connectivity across both local cortical and long-range network levels (Ilmoniemi et al., 1997; Momi et al., 2023), are also systematically modulated by the mu phase at the timing of stimulation (Desideri et al., 2019; Perera et al., 2024). However, most studies only investigated net corticospinal output, meaning the sum of inhibitory and facilitatory processes, by relying solely on single-pulse TMS. As such, we currently only have a limited understanding of the effects of phase on cortical excitability without a clear picture of the contributions of specific intracortical inhibitory and facilitatory circuits.

Paired-pulse transcranial magnetic stimulation (ppTMS) has been widely used to more directly probe intracortical inhibitory and facilitatory dynamics. In particular, short-interval intracortical inhibition (SICI) is thought to reflect GABAergic inhibitory interneuron activity, whereas intracortical facilitation (ICF) is thought to facilitate cortical excitability through activation of glutamatergic excitatory transmission (Cash et al., 2017; Ziemann et al., 2015). These paradigms provide a more direct window

JNeurosci Accepted Manuscript

into intracortical dynamics beyond corticospinal output. Closed-loop EEG-TMS studies have demonstrated phase-dependent modulation of MEPs with spTMS, but evidence for paired-pulse TMS triggered by endogenous oscillatory phase remains limited. SICI has been examined at different phases of the endogenous mu rhythm (Bergmann et al., 2019), whereas ICF has not been tested in this context. SICI and ICF have also been examined at different phases of externally imposed beta tACS (Guerra et al., 2016), and SICI at different phases of alpha tACS (Vallence et al., 2021). However, the externally imposed waveform defines the stimulation phase independently of the ongoing endogenous phase, leaving unresolved whether the spontaneous phase of sensorimotor rhythms similarly modulates these processes.

Here, we test how the specific phase of ongoing brain rhythms shapes responses to SICI and ICF in healthy participants. Using our EEG-guided closed-loop TMS system (Shirinpour et al., 2025), we delivered spTMS, SICI, and ICF at four phases (peak, falling, trough, rising) of ongoing mu and beta rhythms. We measure both MEP and TEP to capture corticospinal and cortical responses, respectively. Both measures showed phase-dependent modulation, with distinct patterns across stimulation conditions, predominantly within the mu rhythm. Notably, responses to SICI and ICF exhibited dissociable phase dependencies, suggesting that they are differentially shaped by oscillatory phase. Our findings advance the understanding of state-dependent cortical circuit dynamics by revealing distinct phase-specific modulation of cortical and corticospinal responses.

JNeurosci Accepted Manuscript

Materials and Methods

Participants

We recruited 24 healthy volunteers (13 female; mean ± SD age: 24.0 ± 7.0 years; range: 18–41 years) in a randomized crossover design, with participants and experimenters blind to the instantaneous phase of stimulation. The sample size (n = 24) was informed by prior closed-loop EEG-TMS studies of phase-dependent corticospinal excitability, which recruited comparable numbers of participants (Wischnewski et al., 2024). Each participant completed two experimental sessions, one targeting mu and the other beta oscillations. Two sessions were separated by at least 48 hours to prevent carryover effects. Session order was randomized across participants. All participants were right-handed and reported no history of neurological or psychiatric disorders, head injuries, or metallic or electrical implants in the head, neck, or chest. Participants were not pre-selected based on electrophysiological characteristics such as resting motor threshold or sensorimotor oscillatory power. The study was approved by the Institutional Review Board of the University of Minnesota, and all participants provided written informed consent prior to participation.

Transcranial magnetic stimulation

We delivered TMS using a MagPro X100 stimulator with a figure-of-eight Cool B-65 coil (MagVenture, Atlanta, GA, USA). The coil was positioned over the left primary motor cortex (M1), targeting the hotspot of the right first dorsal interossei (FDI) muscle. The handle was directed at approximately 45° relative to the midline to induce posterior-to-anterior current flow. The motor hotspot was defined as the coil position eliciting the largest MEP amplitude, and its coordinates were stored and continuously tracked using a Brainsight neuronavigation system (Rogue Research Inc., Montreal, Canada). The resting motor threshold (RMT) was determined at the hotspot using an adaptive threshold-hunting algorithm (Motor Threshold Assessment Tool 2.1) (Awiszus & Borckardt, 2023; Koponen & Peterchev, 2022).

Experimental design

Each session consisted of three blocks, one per stimulation type: spTMS, SICI, and ICF. The order of stimulation blocks was randomized across participants and kept constant across the two sessions

JNeurosci Accepted Manuscript

for each participant. For spTMS, a single suprathreshold pulse was delivered at 120% RMT. For paired-pulse protocols, a conditioning stimulus (CS) at 80% RMT was followed by a test stimulus (TS) at 120% RMT. An inter-stimulus interval (ISI) of 2 ms was used for SICI and 10 ms for ICF, consistent with widely adopted standard protocols (Bergmann et al., 2019; Cash et al., 2017) (Fig. 1*B*). Within each block, 300 trials were delivered at four target phases defined using a cosine-based convention (peak = 0°, falling = 90°, trough = 180°, rising = 270°), applied in a random order. This yielded approximately 75 trials per phase, which was sufficient for reliable MEP measurements (Chang et al., 2016). A jittered inter-trial interval of 2–3 s between consecutive triggers was imposed to minimize carryover effects from preceding pulses. MEPs were recorded from the right FDI using self-adhesive, disposable surface electrodes connected to a BIOPAC ERS100C amplifier (BIOPAC Systems, Inc., Goleta, CA, USA) at a sampling rate of 10 kHz.

EEG acquisition and closed-loop EEG-TMS stimulation

We recorded EEG using a 64-channel TMS-compatible active electrode system (actiCAP slim cap, actiCHamp amplifier; Brain Products GmbH, Gilching, Germany) with electrode positions following the extended 10–20 system. Data were acquired at 10 kHz with 24-bit resolution per channel, and electrode impedances were maintained below 20 kΩ. For closed-loop EEG-TMS, EEG signals were streamed in real time via Lab Streaming Layer to MATLAB (R2020b, MathWorks) and downsampled to 1 kHz. We used the Bayesian Temporal Prediction (BTP) algorithm (Shirinpour et al., 2025) to target four phases of sensorimotor mu (8–13 Hz) and beta (14–30 Hz) (Fig. 1*A*). The phase was extracted from the signal at C3. A Laplacian reference was applied, subtracting the mean of eight surrounding electrodes (FC1, FC3, FC5, C1, C5, CP1, CP3, CP5). Prior to each session, 3 min of resting-state EEG were recorded to train the BTP algorithm. During the training, Bayesian optimization identified individualized prediction parameters that minimized the deviation between the predicted phase and the ground truth based on the rest period. Overlapping data windows were extracted, filtered in the target frequency range, and combinations of prediction parameters (e.g., window length, projection distance) were iteratively tested to estimate the timing of future occurrences of the desired phase. The accuracy of phase targeting was validated by simulating phase predictions on the training data, and the results are reported in Fig. S1. During real-time stimulation, the optimized parameters were used to detect the most recent reliable

JNeurosci Accepted Manuscript

oscillatory anchor point in the incoming EEG and project forward to the desired target phase, accounting for the total system processing delay (Shirinpour et al., 2025). For spTMS, the TMS pulse was delivered at the target phase. For ppTMS protocols (SICI and ICF), the TS was aligned to the target phase. The CS was therefore delivered at an earlier phase, offset by the respective interstimulus interval (2 ms for SICI, 10 ms for ICF).

Data processing and analysis

MEP analysis

Peak-to-peak MEP amplitude was calculated offline using custom MATLAB scripts. MEPs were identified within a window of 20–60 ms after TMS onset. Trials were excluded if the mean absolute EMG activity in the 100 ms preceding the TMS pulse exceeded 0.02 mV and was simultaneously greater than the mean absolute EMG activity plus 2.5 standard deviations of a resting baseline. The resting baseline was defined as the window from 500 to 400 ms before the TMS pulse, following the previous pulse by at least 1500 ms (Wischnewski et al., 2016). All retained MEPs were visually inspected. In total, 2.94% of trials were excluded (2.88% from mu sessions and 3% from beta sessions). Individual MEP amplitudes were log-transformed and then mean-centered within each stimulation block by subtracting the mean log-transformed amplitude of that block.

TEP analysis

EEG data were preprocessed offline using custom scripts in MATLAB with the FieldTrip toolbox (Oostenveld et al., 2011). Two participants were excluded from the TEP analyses because excessive EEG artifacts precluded reliable preprocessing. Preprocessing procedures followed established pipelines for TMS-EEG analysis (Bertazzoli et al., 2021), with modifications tailored to the present experimental design. Data from all three stimulation blocks within a session were concatenated prior to preprocessing. Epochs were first extracted from -500 to +1000 ms relative to TMS onset ($t = 0$), and demeaned. The TMS pulse artifact and early muscle activity were removed by replacing the affected time window with NaN values, followed by interpolation using a cubic Hermite interpolating polynomial (pchip). The artifact window was defined relative to the onset of the first pulse in each stimulation type:

JNeurosci Accepted Manuscript

-5 to +20 ms for spTMS, -7 to +20 ms for SICI (to accommodate the conditioning pulse delivered 2 ms before the test pulse), and -15 to +20 ms for ICF (conditioning pulse at -10 ms). A high-pass filter (1 Hz, 4th-order Butterworth, two-pass) was then applied to remove the DC offset (Bertazzoli et al., 2021).

Noisy trials were identified and rejected automatically based on the z-scored mean absolute amplitude computed over the post-stimulus window (40–1000 ms). Trials in which more than 20% of channels exceeded a z-score threshold of 3 were removed. Bad channels were identified using a correlation-based criterion following the ARTIST method (Wu et al., 2018) and excluded prior to artifact rejection. Independent component analysis (ICA) was then applied to remove residual TMS artifacts, muscle activity, and ocular artifacts using the FastICA algorithm (Bertazzoli et al., 2021). Following artifact removal, the data were band-pass filtered at 1–50 Hz using a fourth-order Butterworth filter, followed by a second ICA. Additional components were removed only when residual artifacts were identified. Bad channels were then interpolated using spline interpolation of neighboring channels on the ICA-cleaned data. Data were then re-referenced to the common average and baseline-corrected using the window from -500 to -10 ms. For statistical analysis, the epoch was cropped to -100 ms to 250 ms.

Trials were sorted by target phase and stimulation type, and phase-specific TEPs were computed by averaging across trials within each condition. TEP waveforms were averaged across a nine-electrode left sensorimotor ROI centered on C3 (C3, C1, C5, FC1, FC3, FC5, CP1, CP3, and CP5). Grand-average P60 and N100 scalp topographies are shown in Fig. S6. We identified the P60 and N100 as the primary TEP components of interest based on cluster-based permutation test results, which consistently identified significant clusters within the P60-N100 latency range across stimulation types. Peak amplitudes for each component were identified per participant within predefined latency windows (P60: 56-85 ms; N100: 86-140 ms). Peak-to-peak amplitude was computed as the difference between P60 and N100 and normalized, separately per stimulation type, by dividing each phase's peak-to-peak amplitude by the participant's mean peak-to-peak amplitude across all four phases.

Statistical analysis

Phase-dependent modulation of MEP amplitude was assessed using a hierarchical generalized linear mixed-effects model (GLMM) approach. First, a full model was run with target phase (peak, falling,

JNeurosci Accepted Manuscript

trough, rising), stimulation type (spTMS, SICI, ICF), and target rhythm (mu, beta) as fixed effects, and participant as a random intercept. Because the full model revealed a significant target rhythm × stimulation type × target phase interaction, subsequent analyses were conducted separately for each rhythm to decompose this interaction. For each rhythm, a GLMM with stimulation type and phase as fixed effects was run, followed by separate GLMMs per stimulation type with phase as the sole fixed effect. Where significant effects were identified, post-hoc pairwise comparisons were performed using two-tailed paired t-tests, with FDR (Benjamini-Hochberg) correction.

For the TEP analysis, phase-dependent modulation of the cortical response was first assessed using a cluster-based permutation test within a repeated-measures ANOVA framework. For each stimulation type, a repeated-measures F-statistic was computed at each time point in the window from 20 to 200 ms, with the four target phases as the within-subject condition. The window began at 20 ms because the TMS pulse artifact was interpolated up to +20 ms. Clusters of temporally contiguous time points exceeding a cluster-forming threshold ($p < 0.05$, based on the F-distribution) were summed to form a cluster-level statistic. A null distribution of maximum cluster masses was generated using 5,000 permutations, in which phase labels were randomly shuffled within each subject. Observed cluster masses were compared against this null distribution to obtain cluster-level p-values (Maris & Oostenveld, 2007). For significant clusters, mean TEP amplitudes within each cluster were computed for each phase condition and compared using paired t-tests. Resulting p-values were corrected for multiple comparisons using FDR across all pairwise phase comparisons. P60, N100, and TEP peak-to-peak amplitudes (P60-N100) were then analyzed using separate GLMMs for each stimulation type and each component, with target phase as a fixed effect and participant as a random intercept. For all analyses, the significance threshold was set at $\alpha = 0.05$. As a check for session-order effects, the primary MEP and TEP GLMMs were refit with session number (first or second visit) as an additional fixed covariate.

To assess the relationship between MEP and TEP phase preferences, we first computed each participant's preferred phase. These analyses were restricted to the 22 participants with usable MEP and TEP data. For each participant, the four normalized amplitude values were assigned to their target phase angles (peak = 0°, falling = 90°, trough = 180°, rising = 270°) and summed as vectors. The angle

JNeurosci Accepted Manuscript

of the summed vector defined the participant's preferred phase, and its length defined the vector length. For each stimulation type, the clustering of preferred phases across participants was tested using Rayleigh's test from the CircStat toolbox (Berens, 2009). The association between MEP and TEP preferred phases across participants was then quantified using a circular-circular correlation coefficient (Berens, 2009). The group mean preferred phase for each stimulation type was computed as the magnitude-weighted circular mean of the individual preferred phases. To assess the sensitivity of the Rayleigh test given the available sample, we report the mean resultant length ($\bar{R}$) as an effect size and performed a Monte Carlo power analysis with 10,000 iterations, in which von Mises distributions were simulated across a range of concentrations to determine the minimum $\bar{R}$ detectable at 80% power at $\alpha = 0.05$.

JNeurosci Accepted Manuscript

Results

Phase-dependent MEP modulation across stimulation conditions

Phase-dependent modulation of MEP amplitude was assessed using a hierarchical GLMM approach. The full model revealed a significant target rhythm × stimulation type × target phase interaction ($F(6,552) = 3.56$, $p = 0.002$; Table 1). Adding session number as a covariate to the full model did not alter this interaction, and session number showed no significant effect (MEP: $F(1,551) = 0.003$, $p = 0.96$; TEP P60-N100: all $p > 0.91$). Subsequent models run separately for each rhythm confirmed significant phase and interaction effects between stimulation type and phase in both mu and beta rhythms (See Table 2). Then, we examined the effect of oscillatory phase for each stimulation type within the mu and beta rhythms. We observed phase-dependent modulation of MEP amplitude across all three stimulation types in the mu rhythm (Fig. 2*A*). ICF yielded the strongest phase effect among the three stimulation types ($F(3,92) = 9.64$, $p < 0.001$), with rising phase eliciting higher amplitudes than peak ($t(23) = -4.70$, $p < 0.001$), falling ($t(23) = -3.29$, $p = 0.010$), and trough ($t(23) = -2.56$, $p = 0.035$), and trough showing higher amplitudes than falling ($t(23) = -2.43$, $p = 0.035$). SICI also showed a significant phase-dependent modulation ($F(3,92) = 6.76$, $p < 0.001$), with peak phase eliciting higher amplitudes than both falling ($t(23) = 3.08$, $p = 0.032$) and trough ($t(23) = 2.62$, $p = 0.046$). spTMS exhibited a significant main effect of phase ($F(3,92) = 5.17$, $p = 0.002$), though pairwise comparisons did not reveal significant differences between specific phase pairs. In the beta rhythm, phase modulation was exclusive to ICF ($F(3,92) = 5.83$, $p = 0.001$), with falling phase showing higher amplitudes than trough ($t(23) = 2.98$, $p = 0.040$). These phase-dependent patterns are further illustrated in the circular plot in Fig. 2*B*. To examine phase-dependent changes in inhibition and facilitation relative to phase-matched spTMS responses, we calculated phase-matched SICI and ICF indices by dividing the conditioned MEP by the spTMS MEP at the corresponding phase (Fig. S5A). To reduce inter-individual differences in overall conditioning magnitude, each participant's indices were normalized to their mean across the four phases. In the mu session, the Index Type × Phase interaction was significant ($F(3,184) = 3.05$, $p = 0.030$). Follow-up analyses showed that the normalized SICI index varied significantly across phase ($F(3,92) = 5.79$, $p = 0.001$), whereas the normalized ICF index did not ($F(3,92) = 0.61$, $p = 0.607$).

JNeurosci Accepted Manuscript

No pairwise comparison for the normalized SICI index remained significant after FDR correction. In the beta session, the Index Type × Phase interaction was not significant ($F(3,184) = 1.25$, $p = 0.293$).

Phase-dependent TEP modulation across stimulation conditions

We examined the effect of oscillatory phase on TEP waveforms using cluster-based permutation tests separately for each stimulation type in both mu and beta sessions. Significant clusters were identified for all three stimulation types in the mu session, spanning portions of the P60-N100 time window (Fig. 3*A*): 42–75 ms (spTMS, $p = 0.007$), 25–72 ms (SICI, $p = 0.002$), 81–112 ms (ICF, $p = 0.016$). In the beta session, no phase-dependent modulation was observed in the early time window; a single significant cluster was identified only for SICI at a later latency (170–195 ms, p = 0.048; Fig. S2). Based on these results, subsequent analyses focused on the mu session. We quantified the P60 and N100 components separately (Fig. 3B), in addition to their peak-to-peak amplitude (Fig. 3C). The P60 component was modulated by phase for spTMS and ICF (spTMS: $F(3,84) = 3.75$, $p = 0.014$; ICF: $F(3,84) = 4.17$, $p = 0.008$), with a comparable trend for SICI ($F(3,84) = 2.61$, $p = 0.057$). The N100 component showed no phase modulation for any stimulation type (spTMS: $F(3,84) = 0.81$, $p = 0.494$; SICI: $F(3,84) = 1.90$, $p = 0.136$; ICF: $F(3,84) = 2.05$, $p = 0.113$). P60-N100 amplitude differed significantly across phases for all three stimulation types (spTMS: $F(3,84) = 5.84$, $p = 0.001$; SICI: $F(3,84) = 5.70$, $p = 0.001$; ICF: $F(3,84) = 6.98$, $p < 0.001$). For SICI, trough and rising phases showed higher amplitudes than peak ($t(21) = -3.73$, $p = 0.008$ and $t(21) = -2.65$, $p = 0.045$, respectively). For ICF, trough and rising phases had higher amplitudes than both peak ($t(21) = -2.76$, $p = 0.035$ and $t(21) = -2.50$, $p = 0.042$, respectively) and falling ($t(21) = -3.11$, $p = 0.032$ and $t(21) = -2.33$, $p = 0.045$, respectively). For spTMS, trough exhibited a higher amplitude than peak ($t(21) = -3.16$, $p = 0.028$). The common-average reference can be influenced by global field changes that may vary across phase conditions. To address this, we performed a sensitivity analysis using an average mastoid reference and observed a broadly consistent phase-dependent modulation of the P60-N100 response across stimulation conditions (Fig. S7), suggesting that our main findings are not attributable to the choice of reference.

JNeurosci Accepted Manuscript

MEP and TEP phase relationships

The phase-dependent modulation of TEP P60-N100 amplitude, summarized as circular representations in Fig. 4*A*, showed preferential responses toward the trough and rising phases across all stimulation types, with ICF exhibiting the most pronounced directional clustering. We then computed each participant's preferred phase for MEP and TEP P60-N100 amplitude using circular vector summation and tested for non-uniform phase distributions using Rayleigh's test (Fig. 4*B*). Across stimulation types, both MEP and TEP showed significant phase preferences, with the exception of SICI-conditioned MEP. The group-level preferred phases are reported in Table 3, and the Rayleigh test results and effect sizes are reported in Table 4. We then assessed the circular correlation between MEP and TEP preferred phases across participants. Only ICF showed a significant correlation between MEP and TEP preferred phases ($R = 0.486$, $p = 0.028$), with mean preferred phases of 263.3° and 223.2°, respectively.

JNeurosci Accepted Manuscript

Discussion

Phase-dependent modulation of corticospinal excitability by sensorimotor mu oscillations has been reported for spTMS (Bergmann et al., 2019; Wischnewski et al., 2022, 2024), although null findings have also been reported (Madsen et al., 2019) and phase can interact with pre-pulse mu power (Suresh & Hussain, 2023). Because spTMS reflects the net corticospinal output of interacting inhibitory and facilitatory processes, the contribution of each process to phase-dependent modulation remains unclear. Here, we demonstrate phase-dependent effects of ppTMS. Specifically, ICF-conditioned responses showed coherent phase-dependent modulation at both the corticospinal and cortical levels, whereas SICI showed phase-dependent cortical responses without a corresponding corticospinal preference, indicating a dissociation between cortical and corticospinal responses.

MEPs elicited by spTMS showed phase-dependent modulation consistent with prior real-time TMS-EEG studies, with larger amplitudes at the trough and rising phase of the mu rhythm (Bergmann et al., 2019; Wischnewski et al., 2022). ICF-conditioned MEPs followed the same phase pattern as those evoked by spTMS, whereas SICI-conditioned MEPs showed the opposite, with the largest amplitudes at the peak phase, indicating that corticospinal responses to the SICI and ICF protocols vary differently across the mu cycle. A phase-matched analysis showed that the normalized SICI index varied across phases, whereas the normalized ICF index did not (Fig. S5A). Thus, the ICF-conditioned response largely preserved the spTMS phase pattern, with a stronger phase effect. This pattern suggests that the phase dependence observed under ICF primarily reflects the underlying phase-dependent corticospinal response rather than phase-dependent modulation of the relative facilitatory effect. Bergmann et al. (2019) found no phase-dependent modulation of SICI, leading them to conclude that mu phase proportionally facilitates both pyramidal cells and inhibitory interneurons, thereby maintaining the excitation-inhibition balance. In contrast, the opposing SICI phase pattern and the phase-dependent variation in the normalized SICI index observed here suggest that the relative inhibitory effect varies across the mu cycle. This discrepancy may arise from differences in phase-targeting approaches, as the present study employed individualized optimization of prediction parameters to improve phase alignment.

JNeurosci Accepted Manuscript

The TS was aligned to the target phase because it evokes the MEP and provides a common phase reference across stimulation types. With a fixed ISI, the realized CS and TS phases are coupled and differ by a near-constant offset (Fig. S3). Conditioned MEPs were analyzed separately with respect to the realized CS and TS phases. The modulation amplitude was preserved between references, while the phase angle shifted by the corresponding offset. Phase dependence of SICI- and ICF-conditioned responses in the mu session remained significant under both references (Fig. S4, Table S1). Thus, the two references describe the same modulation viewed from a shifted phase origin rather than independent effects. A previous study aligned the CS to externally imposed tACS phase but noted that the similar phase dependencies of single-pulse and ICF responses made it difficult to exclude an effect on the TS response (Guerra et al., 2016). Aligning the CS therefore does not isolate CS-phase effects from TS-phase effects, and the present results establish phase-dependent modulation of the conditioned response with respect to the CS–TS pulse pair without determining whether it is driven by the CS phase, the TS phase, or their interaction.

Phase-dependent TEP modulation was observed across all stimulation types in the mu session, with P60-N100 peak-to-peak amplitude greatest at the trough and rising phases. We initially quantified the P60-N100 amplitude as a measure that is less sensitive to inter-individual baseline variability, providing a more stable estimate of overall TEP amplitude. The convergence of this modulation across stimulation types suggests that the oscillatory phase broadly influences cortical responses to both single- and paired-pulse stimulation. To further examine the underlying contributions, we analyzed P60 and N100 separately. P60 is commonly associated with early excitatory inputs, whereas N100 has been linked to GABAergic inhibition and the cortical silent period (Premoli et al., 2018). The observed phase dependency was more closely reflected in the P60 component than in the N100 component, which may be consistent with a greater contribution of processes associated with early excitatory activity (Fig. 3B).

In the ICF condition, cortical and corticospinal responses showed partially corresponding phase-dependent patterns. MEP and TEP preferred phases each showed significant clustering across participants (Rayleigh's tests, $p < 0.05$), and their significant circular correlation indicated that cortical and corticospinal responses under the ICF protocol are linked in their phase dependence. By contrast, spTMS-evoked MEP and TEP showed divergent preferred phases at the individual level despite similar

JNeurosci Accepted Manuscript

group-level patterns, consistent with a previous study, reporting overlapping phase preferences between cortical and corticospinal responses under spTMS (Perera et al., 2024). For SICI, the TEP followed a similar phase pattern to ICF and spTMS, whereas the SICI-conditioned MEPs showed an opposing pattern, with larger amplitudes around the peak phase. Although SICI-conditioned MEP amplitude varied significantly across phases at the group level, individual preferred phases did not significantly cluster in the Rayleigh test. The GLMM assesses amplitude differences across phases, whereas the Rayleigh test assesses alignment of individual preferred phases. Thus, group-level phase-dependent modulation can be present even when preferred phases are not strongly aligned across participants. Sensitivity analysis indicated that the Rayleigh test could reliably detect clustering only for effect sizes ($\bar{R}$) above 0.45 (80% power), whereas the observed effect size for SICI-conditioned MEPs was 0.26. Therefore, the non-significant clustering is inconclusive regarding the presence of a shared preferred phase. The relatively modest magnitudes of the group-level vectors indicate that the corresponding mean directions should not be interpreted as strongly shared biological phase preferences, as they may reflect weak within-participant modulation, heterogeneity in preferred phase, or both.

Phase-dependent modulation was weaker and less consistent in the beta session. Only ICF-conditioned MEPs showed a significant phase effect, limited to a single pairwise comparison (falling > trough), and TEP amplitude was not significantly modulated by beta phase for any stimulation type. These results are consistent with prior work showing that beta phase targeting produces smaller effect sizes than mu in both MEP and TEP outcomes (Perera et al., 2024; Wischnewski et al., 2022). Resting-state SNR was significantly higher for mu than for beta (Fig. S5B), consistent with the broader bandwidth and reduced stationarity of the beta band, which make reliable real-time phase targeting more challenging (Shirinpour et al., 2025; Wischnewski et al., 2024). Consistent with this, phase targeting accuracy was lower in the beta session than in the mu session across all stimulation types (Fig. S1). A trial-count subsampling analysis further showed that beta effect sizes for spTMS and SICI remained low regardless of trial count (Fig. S5C), indicating that the weaker beta modulation is unlikely to reflect insufficient trial counts alone. The realized-phase analysis also showed no significant phase modulation in the beta session, suggesting that the weaker beta-band effects are unlikely to be

JNeurosci Accepted Manuscript

explained by targeting inaccuracy alone, although the present data cannot establish the absence of a true beta-band modulation. The phase-dependent corticospinal modulation observed here parallels recent findings across thalamocortical sleep spindle phase (Hassan et al., 2025), raising the possibility that such phase-dependent modulation is a general property of thalamocortical alpha-band rhythms rather than a wake-specific phenomenon. Whether distinct cortical and corticospinal phase patterns also arise during spindle-phase-triggered ppTMS remains an open question for future work.

Several limitations should be considered. First, the TEP components reflect a compound response to both the conditioning and test stimuli, and no conditioning-only condition was recorded. However, the paired-pulse response does not necessarily reflect the passive summation of the two individual responses. A comparable paradigm found that the paired-pulse TEP differed from the linear sum of the separately recorded conditioning- and test-evoked responses (Ferreri et al., 2011). We therefore interpret the TEP effects as reflecting the combined cortical response to paired-pulse stimulation, without assigning them to specific inhibitory or facilitatory circuits. Next, auditory masking and dedicated coil-click or scalp-sensation controls were not included. However, the coil, pulse parameters, and hardware were identical across phase conditions, and target phases were randomized. Sensory potentials were therefore consistent across conditions, and the observed phase effects are unlikely to be related to them. While a contribution from sensory-evoked activity to the TEPs cannot be excluded, this sensory activity is more likely to affect later components (> 100 ms) (Biabani et al., 2019; Murphy et al., 2024). The suprathreshold test pulse at 120% RMT may have attenuated phase-dependent MEP modulation, as phase effects have been reported to be stronger at lower stimulation intensities (Schaworonkow et al., 2019). However, phase modulation remained detectable for ICF under the suprathreshold stimulation protocol. It would be informative for future studies to examine whether the phase dependence of ppTMS varies across test-pulse intensities. The sample was limited to young, healthy, and right-handed adults. Future studies in older adults and clinical populations will therefore be needed to determine whether the observed protocol-specific phase patterns generalize more broadly.

Oscillatory phase plays an important role in shaping corticospinal excitability, and our findings extend phase-dependent TMS effects from single-pulse to paired-pulse stimulation. These findings may

JNeurosci Accepted Manuscript

inform future efforts to optimize state-dependent stimulation in clinical conditions associated with altered cortical excitation-inhibition balance.

JNeurosci Accepted Manuscript

References

Awiszus, F., & Borckardt, J. (2023). *TMS motor threshold assessment tool* (Version 2.1) [Computer software]. https://www.clinicalresearcher.org/software.htm

Berens, P. (2009). **CircStat**: A *MATLAB* Toolbox for Circular Statistics. *Journal of Statistical Software*, *31*(10). https://doi.org/10.18637/jss.v031.i10

Bergmann, T. O., Lieb, A., Zrenner, C., & Ziemann, U. (2019). Pulsed Facilitation of Corticospinal Excitability by the Sensorimotor μ-Alpha Rhythm. *The Journal of Neuroscience*, *39*(50), 10034–10043. https://doi.org/10.1523/JNEUROSCI.1730-19.2019

Bertazzoli, G., Esposito, R., Mutanen, T. P., Ferrari, C., Ilmoniemi, R. J., Miniussi, C., & Bortoletto, M. (2021). The impact of artifact removal approaches on TMS–EEG signal. *NeuroImage*, *239*, 118272. https://doi.org/10.1016/j.neuroimage.2021.118272

Biabani, M., Fornito, A., Mutanen, T. P., Morrow, J., & Rogasch, N. C. (2019). Characterizing and minimizing the contribution of sensory inputs to TMS-evoked potentials. *Brain Stimulation*, *12*(6), 1537–1552. https://doi.org/10.1016/j.brs.2019.07.009

Buzsáki, G., & Draguhn, A. (2004). Neuronal Oscillations in Cortical Networks. *Science*, *304*(5679), 1926–1929. https://doi.org/10.1126/science.1099745

Cash, R. F. H., Noda, Y., Zomorrodi, R., Radhu, N., Farzan, F., Rajji, T. K., Fitzgerald, P. B., Chen, R., Daskalakis, Z. J., & Blumberger, D. M. (2017). Characterization of Glutamatergic and GABAA-Mediated Neurotransmission in Motor and Dorsolateral Prefrontal Cortex Using Paired-Pulse TMS–EEG. *Neuropsychopharmacology*, *42*(2), 502–511. https://doi.org/10.1038/npp.2016.133

Chang, W. H., Fried, P. J., Saxena, S., Jannati, A., Gomes-Osman, J., Kim, Y.-H., & Pascual-Leone, A. (2016). Optimal number of pulses as outcome measures of neuronavigated

JNeurosci Accepted Manuscript

transcranial magnetic stimulation. *Clinical Neurophysiology*, *127*(8), 2892–2897. https://doi.org/10.1016/j.clinph.2016.04.001

Chen, L. L., Madhavan, R., Rapoport, B. I., & Anderson, W. S. (2013). Real-Time Brain Oscillation Detection and Phase-Locked Stimulation Using Autoregressive Spectral Estimation and Time-Series Forward Prediction. *IEEE Transactions on Biomedical Engineering*, *60*(3), 753–762. https://doi.org/10.1109/TBME.2011.2109715

Desideri, D., Zrenner, C., Ziemann, U., & Belardinelli, P. (2019). Phase of sensorimotor μ-oscillation modulates cortical responses to transcranial magnetic stimulation of the human motor cortex. *The Journal of Physiology*, *597*(23), 5671–5686. https://doi.org/10.1113/JP278638

Donoghue, T., Haller, M., Peterson, E. J., Varma, P., Sebastian, P., Gao, R., Noto, T., Lara, A. H., Wallis, J. D., Knight, R. T., Shestyuk, A., & Voytek, B. (2020). Parameterizing neural power spectra into periodic and aperiodic components. *Nature Neuroscience*, *23*(12), 1655–1665. https://doi.org/10.1038/s41593-020-00744-x

Dugué, L., Marque, P., & VanRullen, R. (2011). The Phase of Ongoing Oscillations Mediates the Causal Relation between Brain Excitation and Visual Perception. *The Journal of Neuroscience*, *31*(33), 11889–11893. https://doi.org/10.1523/JNEUROSCI.1161-11.2011

Ferreri, F., Pasqualetti, P., Määttä, S., Ponzo, D., Ferrarelli, F., Tononi, G., Mervaala, E., Miniussi, C., & Rossini, P. M. (2011). Human brain connectivity during single and paired pulse transcranial magnetic stimulation. *NeuroImage*, *54*(1), 90–102. https://doi.org/10.1016/j.neuroimage.2010.07.056

Guerra, A., Pogosyan, A., Nowak, M., Tan, H., Ferreri, F., Di Lazzaro, V., & Brown, P. (2016). Phase Dependency of the Human Primary Motor Cortex and Cholinergic Inhibition Cancelation During Beta tACS. *Cerebral Cortex*, *26*(10), 3977–3990. https://doi.org/10.1093/cercor/bhw245

JNeurosci Accepted Manuscript

Haigh, Z. J., Tran, H., Berger, T., Shirinpour, S., Alekseichuk, I., Koenig, S., Zimmermann, J., McGovern, R., Darrow, D., Herman, A., Wischnewski, M., & Opitz, A. (2025). Modulation of motor excitability reflects traveling waves of neural oscillations. *Cell Reports*, *44*(6), 115864. https://doi.org/10.1016/j.celrep.2025.115864

Hassan, U., Okyere, P., Masouleh, M. A., Zrenner, C., Ziemann, U., & Bergmann, T. O. (2025). Pulsed inhibition of corticospinal excitability by the thalamocortical sleep spindle. *Brain Stimulation*, *18*(2), 265–275. https://doi.org/10.1016/j.brs.2025.02.015

Ilmoniemi, R. J., Virtanen, J., Ruohonen, J., Karhu, J., Aronen, H. J., Näätänen, R., & Katila, T. (1997). Neuronal responses to magnetic stimulation reveal cortical reactivity and connectivity: *NeuroReport*, *8*(16), 3537–3540. https://doi.org/10.1097/00001756-199711100-00024

Koponen, L. M., & Peterchev, A. V. (2022). Preventing misestimation of transcranial magnetic stimulation motor threshold with MTAT 2.0. *Brain Stimulation*, *15*(5), 1073–1076. https://doi.org/10.1016/j.brs.2022.07.057

Madsen, K. H., Karabanov, A. N., Krohne, L. G., Safeldt, M. G., Tomasevic, L., & Siebner, H. R. (2019). No trace of phase: Corticomotor excitability is not tuned by phase of pericentral mu-rhythm. *Brain Stimulation*, *12*(5), 1261–1270. https://doi.org/10.1016/j.brs.2019.05.005

Maris, E., & Oostenveld, R. (2007). Nonparametric statistical testing of EEG- and MEG-data. *Journal of Neuroscience Methods*, *164*(1), 177–190. https://doi.org/10.1016/j.jneumeth.2007.03.024

Momi, D., Wang, Z., & Griffiths, J. D. (2023). TMS-evoked responses are driven by recurrent large-scale network dynamics. *eLife*, *12*, e83232. https://doi.org/10.7554/eLife.83232

Murphy, D. L. K., Koponen, L. M., Wood, E., Li, Y., Bukhari-Parlakturk, N., Goetz, S. M., & Peterchev, A. V. (2024). Reduced auditory perception and brain response with quiet

JNeurosci Accepted Manuscript

TMS coil. *Brain Stimulation*, *17*(6), 1197–1207. https://doi.org/10.1016/j.brs.2024.10.003

Oostenveld, R., Fries, P., Maris, E., & Schoffelen, J.-M. (2011). FieldTrip: Open Source Software for Advanced Analysis of MEG, EEG, and Invasive Electrophysiological Data. *Computational Intelligence and Neuroscience*, *2011*, 1–9. https://doi.org/10.1155/2011/156869

Perera, N. D., Wischnewski, M., Alekseichuk, I., Shirinpour, S., & Opitz, A. (2024). State-Dependent Motor Cortex Stimulation Reveals Distinct Mechanisms for Corticospinal Excitability and Cortical Responses. *Eneuro*, *11*(11), ENEURO.0450-24.2024. https://doi.org/10.1523/ENEURO.0450-24.2024

Premoli, I., Király, J., Müller-Dahlhaus, F., Zipser, C. M., Rossini, P., Zrenner, C., Ziemann, U., & Belardinelli, P. (2018). Short-interval and long-interval intracortical inhibition of TMS-evoked EEG potentials. *Brain Stimulation*, *11*(4), 818–827. https://doi.org/10.1016/j.brs.2018.03.008

Schaworonkow, N., Triesch, J., Ziemann, U., & Zrenner, C. (2019). EEG-triggered TMS reveals stronger brain state-dependent modulation of motor evoked potentials at weaker stimulation intensities. *Brain Stimulation*, *12*(1), 110–118. https://doi.org/10.1016/j.brs.2018.09.009

Shirinpour, S., Alekseichuk, I., Güth, M. R., Haigh, Z., Wischnewski, M., & Opitz, A. (2025). Bayesian Temporal Prediction: A Robust Algorithm for Real-Time EEG Phase-Dependent Brain Stimulation. *IEEE Transactions on Biomedical Engineering*, *73*(2), 611–620. https://doi.org/10.1109/TBME.2025.3589970

Shirinpour, S., Alekseichuk, I., Mantell, K., & Opitz, A. (2020). Experimental evaluation of methods for real-time EEG phase-specific transcranial magnetic stimulation. *Journal of Neural Engineering*, *17*(4), 046002. https://doi.org/10.1088/1741-2552/ab9dba

JNeurosci Accepted Manuscript

Siebner, H. R., Funke, K., Aberra, A. S., Antal, A., Bestmann, S., Chen, R., Classen, J., Davare, M., Di Lazzaro, V., Fox, P. T., Hallett, M., Karabanov, A. N., Kesselheim, J., Beck, M. M., Koch, G., Liebetanz, D., Meunier, S., Miniussi, C., Paulus, W., … Ugawa, Y. (2022). Transcranial magnetic stimulation of the brain: What is stimulated? – A consensus and critical position paper. *Clinical Neurophysiology*, *140*, 59–97. https://doi.org/10.1016/j.clinph.2022.04.022

Suresh, T., & Hussain, S. J. (2023). Re-evaluating the contribution of sensorimotor mu rhythm phase and power to human corticospinal output: A replication study. *Brain Stimulation*, *16*(3), 936–938. https://doi.org/10.1016/j.brs.2023.05.022

Vallence, A., Dansie, K., Goldsworthy, M. R., McAllister, S. M., Yang, R., Rothwell, J. C., & Ridding, M. C. (2021). Examining motor evoked potential amplitude and short-interval intracortical inhibition on the up-going and down-going phases of a transcranial alternating current stimulation (tacs) imposed alpha oscillation. *European Journal of Neuroscience*, *53*(8), 2755–2762. https://doi.org/10.1111/ejn.15124

Wischnewski, M., Haigh, Z. J., Shirinpour, S., Alekseichuk, I., & Opitz, A. (2022). The phase of sensorimotor mu and beta oscillations has the opposite effect on corticospinal excitability. *Brain Stimulation*, *15*(5), 1093–1100. https://doi.org/10.1016/j.brs.2022.08.005

Wischnewski, M., Kowalski, G. M., Rink, F., Belagaje, S. R., Haut, M. W., Hobbs, G., & Buetefisch, C. M. (2016). Demand on skillfulness modulates interhemispheric inhibition of motor cortices. *Journal of Neurophysiology*, *115*(6), 2803–2813. https://doi.org/10.1152/jn.01076.2015

Wischnewski, M., Shirinpour, S., Alekseichuk, I., Lapid, M. I., Nahas, Z., Lim, K. O., Croarkin, P. E., & Opitz, A. (2024). Real-time TMS-EEG for brain state-controlled research and precision treatment: A narrative review and guide. *Journal of Neural Engineering*, *21*(6), 061001. https://doi.org/10.1088/1741-2552/ad8a8e

JNeurosci Accepted Manuscript

Wu, W., Keller, C. J., Rogasch, N. C., Longwell, P., Shpigel, E., Rolle, C. E., & Etkin, A. (2018). ARTIST: A fully automated artifact rejection algorithm for single-pulse TMS-EEG data. *Human Brain Mapping*, *39*(4), 1607–1625. https://doi.org/10.1002/hbm.23938

Ziemann, U., Reis, J., Schwenkreis, P., Rosanova, M., Strafella, A., Badawy, R., & Müller-Dahlhaus, F. (2015). TMS and drugs revisited 2014. *Clinical Neurophysiology*, *126*(10), 1847–1868. https://doi.org/10.1016/j.clinph.2014.08.028

Zrenner, C., Desideri, D., Belardinelli, P., & Ziemann, U. (2018). Real-time EEG-defined excitability states determine efficacy of TMS-induced plasticity in human motor cortex. *Brain Stimulation*, *11*(2), 374–389. https://doi.org/10.1016/j.brs.2017.11.016

JNeurosci Accepted Manuscript

Figure legends

Figure 1. Schematic of the closed-loop EEG-TMS experiment. ***A,*** The BTP algorithm continuously processes the Laplacian-filtered EEG signal at C3 (blue dot), located over the left M1 hand area, computed from surrounding electrodes (black dots), to predict the upcoming phase of the oscillation and trigger TMS at one of four target phases: peak (0°), falling (90°), trough (180°), or rising (270°). ***B,*** Stimulation protocols. For spTMS, a single suprathreshold pulse was delivered at 120% RMT. For SICI and ICF, a subthreshold conditioning pulse (CS) at 80% RMT preceded the test pulse (TS) by 2 ms and 10 ms, respectively.

Figure 2. Phase-dependent modulation of normalized log-transformed MEP amplitude across stimulation types. ***A,*** Group average (n = 24) ± standard error of the mean (SEM) for spTMS (grey), SICI (red), and ICF (blue) across oscillatory phases in the mu (left) and beta (right) sessions. Asterisks indicate significant pairwise differences (p < 0.05, FDR-corrected). ***B,*** Polar plot representation of phase-dependent MEP patterns across stimulation types for the mu (left) and beta (right) sessions. Each dot represents the group mean of normalized log-transformed MEP amplitude for each phase condition, and the shaded area indicates ± SEM. The radial axis represents the normalized log-transformed MEP amplitude.

Figure 3. Phase-dependent modulation of TEP amplitude across stimulation types in the mu session. ***A,*** Grand-average TEP waveforms across oscillatory phases (peak, falling, trough, rising) for spTMS (top), SICI (middle), and ICF (bottom). Shaded areas represent the standard error of the mean. Dark gray shading indicates the TMS artifact interpolation window. Light gray shading and asterisks indicate significant clusters identified by cluster-based permutation tests (p < 0.05). ***B,*** P60 (green) and N100 (pink) amplitudes across oscillatory phases for spTMS (top), SICI (middle), and ICF (bottom). ***C,*** Normalized P60-N100 peak-to-peak amplitude across oscillatory phases for spTMS (top), SICI (middle), and ICF (bottom). Error bars represent the standard error of the mean. Asterisks in B and C indicate significant pairwise differences (p < 0.05, FDR-corrected).

JNeurosci Accepted Manuscript

Figure 4. Phase preference of MEP and TEP P60-N100 amplitude in the mu session. ***A,*** Circular representation of phase-dependent TEP P60-N100 modulation across stimulation types (spTMS, gray; SICI, red; ICF, blue). ***B,*** Individual preferred phases for MEP (orange) and TEP P60-N100 (colored by stimulation type) for spTMS (left), SICI (middle), and ICF (right). Each dot represents one participant. Arrows indicate the group mean preferred phase for MEP and TEP P60-N100 within each stimulation type; arrow length is fixed and does not encode magnitude. The group mean vector length for each stimulation type is reported in Table 3. Asterisks indicate significant phase preferences (Rayleigh's test, $p < 0.05$). Phase angles are defined as peak = 0°, falling = 90°, trough = 180°, rising = 270°.

JNeurosci Accepted Manuscript.

Table

Table 1. GLMM results for phase-dependent MEP modulation: target rhythm × stimulation type × target phase interaction.

Factor	*F*	*df1*	*df2*	*p*
Target rhythm	13.82	1	552	< 0.001
Stimulation type	1.05	2	552	0.351
Target phase	2.68	3	552	0.046
Target rhythm × stimulation type	2.14	2	552	0.118
Target rhythm × target phase	6.95	3	552	< 0.001
Stimulation type × target phase	2.43	6	552	0.025
Target rhythm × stimulation type × target phase	3.56	6	552	0.002

Table 2. GLMM results for phase-dependent MEP modulation by target rhythm: stimulation type × target phase interaction.

Frequency	Factor	*F*	*df1*	*df2*	*p*
Mu	Stimulation type	0.99	2	276	0.374
Mu	Target phase	6.96	3	276	< 0.001
Mu	Stimulation type × target phase	4.18	6	276	< 0.001
Beta	Stimulation type	1.38	2	276	0.254
Beta	Target phase	3.51	3	276	0.016
Beta	Stimulation type × target phase	3.18	6	276	0.005

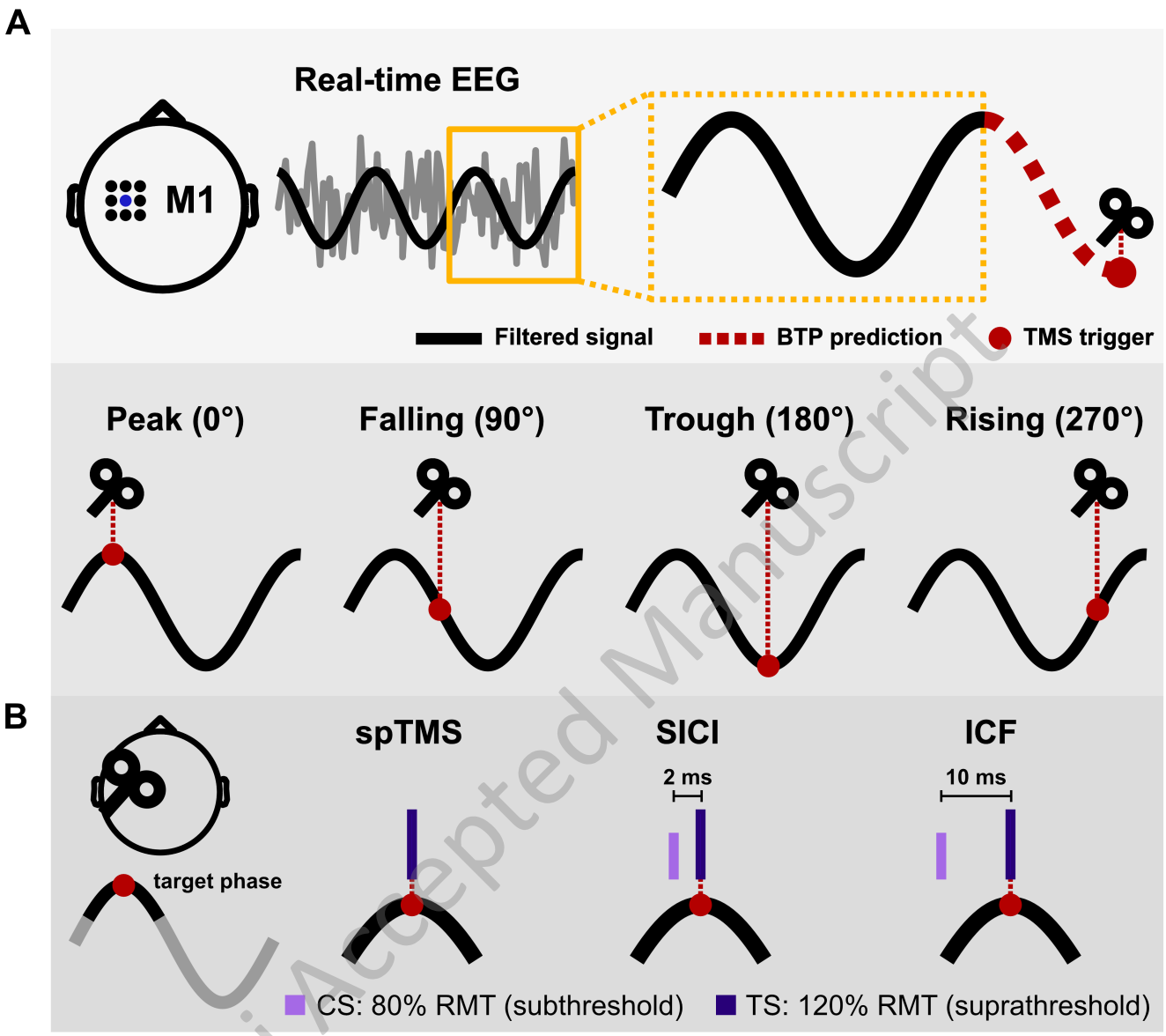
Table 3. Group-level preferred phase and vector length for MEP and TEP responses by stimulation type (mu rhythm).

Stimulation type	MEP mean angle (°)	TEP mean angle (°)	MEP vector length	TEP vector length
spTMS	252.5	193.3	0.175	0.201
SICI	330.7	196.3	0.187	0.225
ICF	263.3	223.2	0.174	0.217

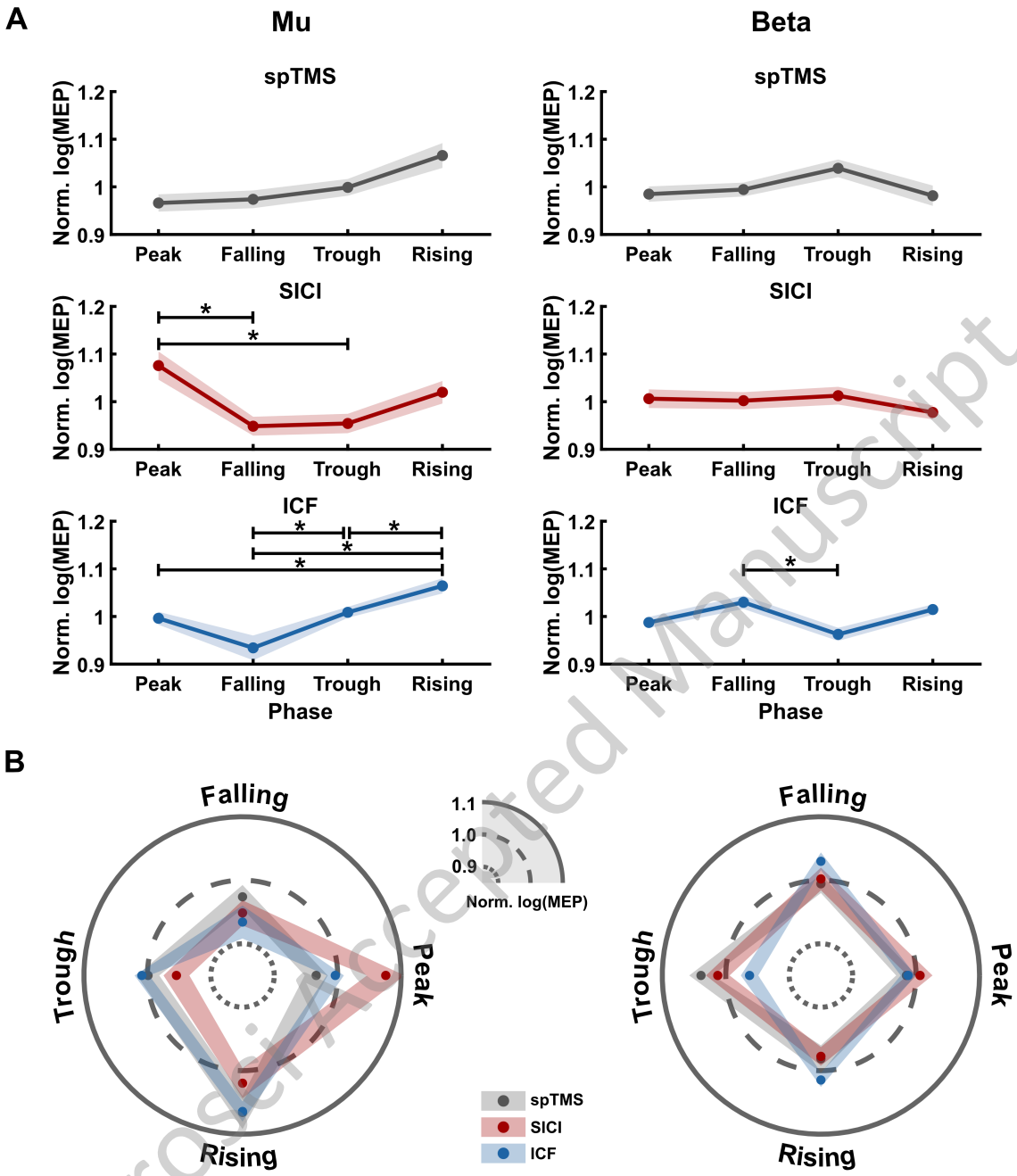
Table 4. Effect size ($\bar{R}$) and Rayleigh test results for MEP and TEP preferred phases (mu rhythm).

Stimulation type	MEP $\bar{R}$	MEP *p*	TEP $\bar{R}$	TEP *p*
spTMS	0.383	0.038	0.478	0.005
SICI	0.263	0.221	0.473	0.006
ICF	0.629	< 0.001	0.446	0.011

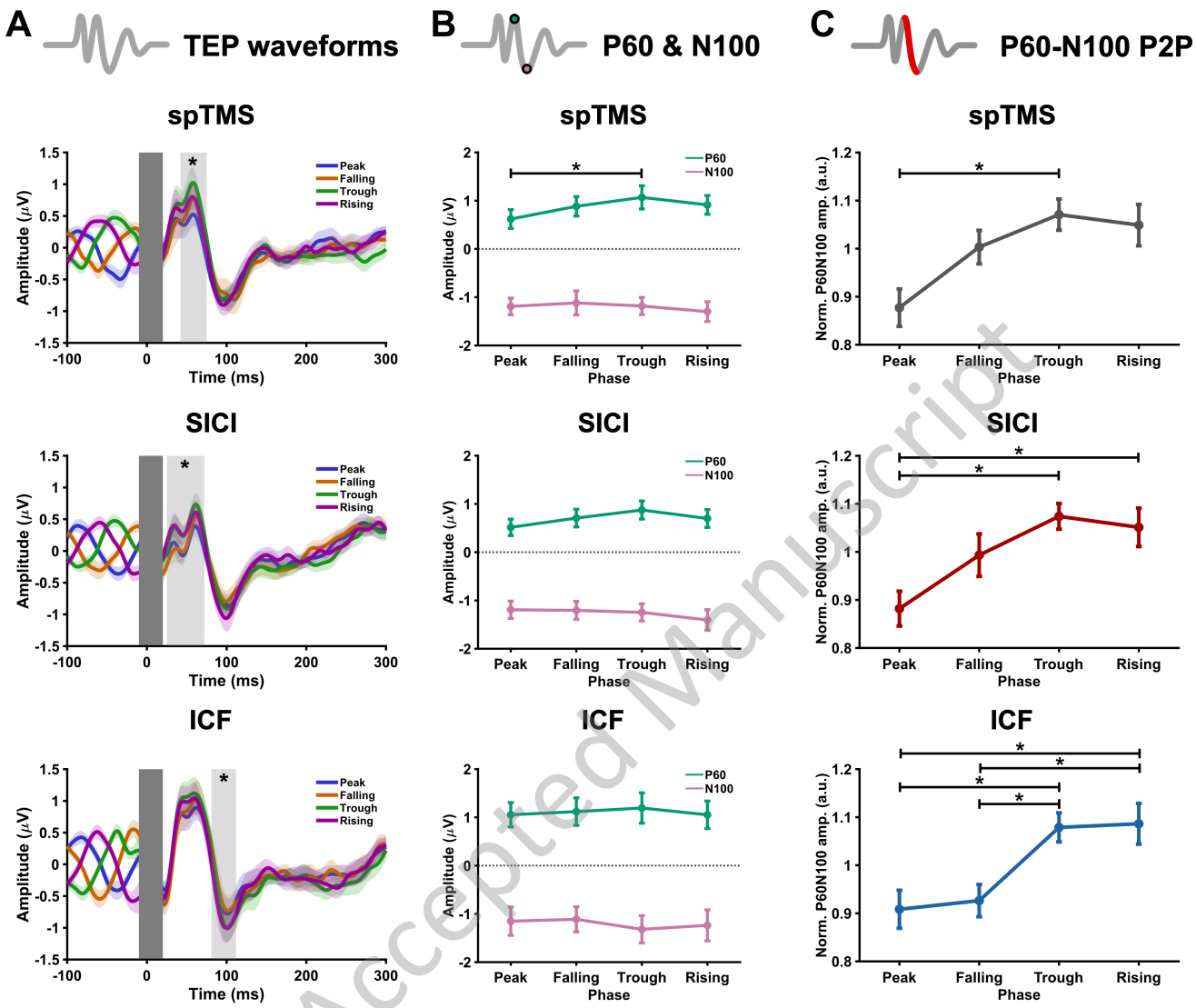
JNeurosci Accepted Manuscript



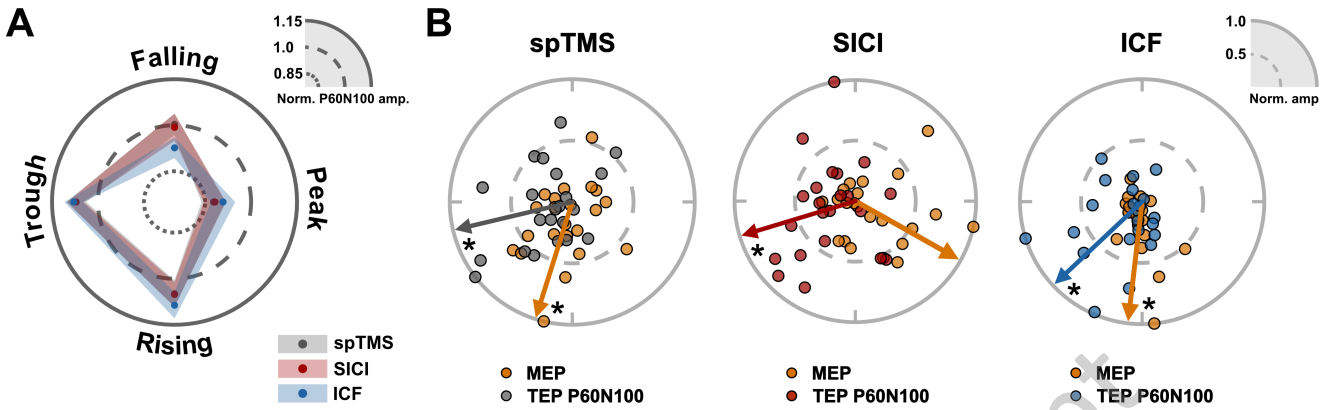
JNeurosci Accepted Manuscript



JNeurosci Accepted Manuscript



JNeurosci Accepted Manuscript



JNeurosci Accepted Manuscript